



Delineation of groundwater aquifers using VES and 2D imaging techniques in north Badra area, Eastern Iraq

Jassim M. Thabit^{1*}, Mohammed M. AL-Hameedawie²

¹Department of Geology, College of Science, University of Baghdad. Baghdad, Iraq

²The General Commission for Groundwater, Baghdad, Iraq.

Abstract:

The resistivity survey was carried out by using vertical electrical sounding (VES) and 2D imaging techniques in the northern Badra area, Eastern Iraq. Eleven VES points distributed on two parallel profiles and six 2D imaging stations were applied using long survey lines.

In general, two types of aquifers are recognized in the study area. The first is the Quaternary aquifer, which appears in all geological sections and inverse model of 2D imaging stations (2DS). This aquifer can be divided into upper and lower aquifers as shown in (2DS1), (2DS3), and (2DS4). Generally, the thickness of this aquifer ranges between (30-200 m) which occurs at a depth of (10-30m) according to geological sections, while its thickness ranges between (35-180m) and occurs at depth (10-45m) according to the inverse model of 2D imaging stations. The second is the AL-Mukdadiya aquifer, which appears only in 2DS1 at a depth of (140m), and its thickness is more than (80m).

The comparison between VES and 2D imaging techniques revealed that the VES technique is the best in delineating the boundaries between layers. However, the 2D imaging technique is better at delineating the aquifers, and at determining the vertical and horizontal changes in resistivity within layers and aquifers, and it also succeeded in recognizing the upper and lower aquifers of quaternary aquifer as shown in (2DS1), (2DS3), and (2DS4). Therefore, 2D imaging is better at recognizing more layers or aquifers than that of VES technique, especially with the gradual decrease (or increase) in resistivity values or layers with small thickness. Also, the VES technique showed a high depth of investigation (DOI) in comparison with 2D imaging technique.

Keyword: Vertical Electrical Sounding (VES), 2D imaging technique, Aquifer delineation.

تحديد خزانات المياه الجوفية باستخدام تقنية الجس العمودي الكهربائي و تقنية ثنائي البعد في شمال منطقة بدر، شرق العراق

د. جاسم محمد ثابت^{1*}، محمد محسن الحميداوي²

¹قسم علم الارض، كلية العلوم، جامعة بغداد، ²الهيئة العامة للمياه الجوفية، بغداد، العراق

الخلاصة:

أجري مسح للمقاومة النوعية باستخدام الجس الكهربائي العمودي (VES) و تقنية ثنائي البعد في شمال منطقة بدر، شرق العراق، اذ بلغ عدد نقاط الجس الكهربائي العمودي (11) نقطة موزعة على مسارين متوازيين. اما محطات ثنائي البعد فقد كان عددها (6). تم تمييز نوعين من خزانات المياه الجوفية في منطقة

*Email: jassimthabit@yahoo.com

الدراسة. الاول يمثل ترسبات العصر الرباعي و الذي ظهر في جميع المقاطع الجيولوجية للجس الكهربائي العمودي و موديلات المحطات الثنائية البعد. هذا الخزان يمكن ان ينقسم الى خزان علوي و خزان سفلي كما ظهر في محطات ثنائية البعد (2DS1), (2DS3), (2DS4). يتراوح سمك هذا الخزان بين (30-200م) و بعمق (10-30م) اعتماداً على المقاطع الجيولوجية بينما تتراوح سمكة بين (35-180م) و بعمق (10-45م) اعتماداً على المحطات ثنائية البعد. الخزان الثاني هو خزان المقدادية و الذي ظهر فقط في محطة القياس (2DS1) على عمق (140م) و بسمك اكثر من (80م).
 أظهرت المقارنة ان تقنية الجس الكهربائي العمودي كانت الافضل في تحديد الحدود بين الطبقات و لكن تقنية ثنائي البعد كانت افضل في تحديد الخزانات الجوفية و التغيرات في المقاومة ضمن الخزانات الجوفية و تحديد التغير العمودي و الافقي في المقاومة، لذلك فان تقنية ثنائي البعد هي افضل من تقنية الجس الكهربائي العمودي في تمييز الطبقات و الخزانات الجوفية و خاصة عند وجود نقصان او زيادة تدريجية في قيم المقاومة او عند وجود طبقات ذات سمك قليل. كذلك فان تقنية الجس الكهربائي اعطت عمق تحري اكبر من تقنية ثنائي البعد.

Introduction

In recent decades, the electrical resistivity method has been developed rapidly. The one dimensional (1D) resistivity technique was used in the pioneer works of Conrand Schlumberger [1, 2], where Vertical Electrical Sounding (VES) was the most used in this technique using Schlumberger array. The major development of electrical resistivity method in the last 20 year is the two dimensional (2D) and three dimensional (3D) imaging techniques using common electrode arrays such as Pole-Pole, Pole-Dipole, Dipole-Dipole, Wenner Schlumberger, Wenner, and Gradient arrays [3-11].

A lot of literature used the VES and/or 2D techniques to delineate groundwater aquifers such as [12-21]. Other literatures such as [22, 23] used VES and 2D techniques together to delineate aquifers and make comparisons between them. They concluded that the 2D imaging technique can give better lateral view of subsurface layers than VES technique. Also, [23] found that the 2D imaging is the best in delineating shallow aquifers.

The study area is located within the Wasit province in the northern Badra area, Eastern Iraq. It is bounded between latitude ($33^{\circ} 17' - 33^{\circ} 07'$) north, and longitude ($45^{\circ} 53' - 46^{\circ} 04'$) east. The major part of the study area is flat, reflecting the Mesopotamian zone. The area slopes gradually southwest, where the highest point reaches (140m) and the lowest point is (50m) above sea level.

Geologically, the Quaternary deposits cover most of the study area. They are basically alluvial fans. These fans consist of poorly sorted clastics deposits. The Quaternary deposits are gravel, sand, silt, clay and secondary gypsum within sand deposits near the surface, figure 1-. According to wells drilled in the Quaternary deposits, the thickness of these deposits exceeds (100m), and it increases toward the west and southwest [24].

The Quaternary deposits are unconsolidated and usually finer grained than the under laying pebbly sandstone of AL-Mukdadiya Formation [25].

AL-Mukdadiya Formation (Late Miocene) is comprised of fining upward cycles of pebbly sandstone, sandstone, and red mudstone [25]. In the study area, this Formation is exposed in the east Badra area [26].

Two types of aquifers are present within the study area: confined aquifer represented by AL-Mukdadiya Formation and unconfined aquifer represented by Quaternary deposits [27, 28].

The TDS of groundwater is between (2500-4000 ppm). It reaches 9600 ppm in well (BH5). However, the lithology of six wells (BH) is used as a reference to compare with the 1D and 2D results.

The aim of this study is to delineate groundwater aquifers in complex sedimentary deposits using VES and 2D imaging techniques, and to compare them to show the best in determining the aquifers especially at depths of more than 100 m. So, it will take the use of the long survey lines for VES and 2D techniques to delineate the deep aquifers in complex sedimentary areas.

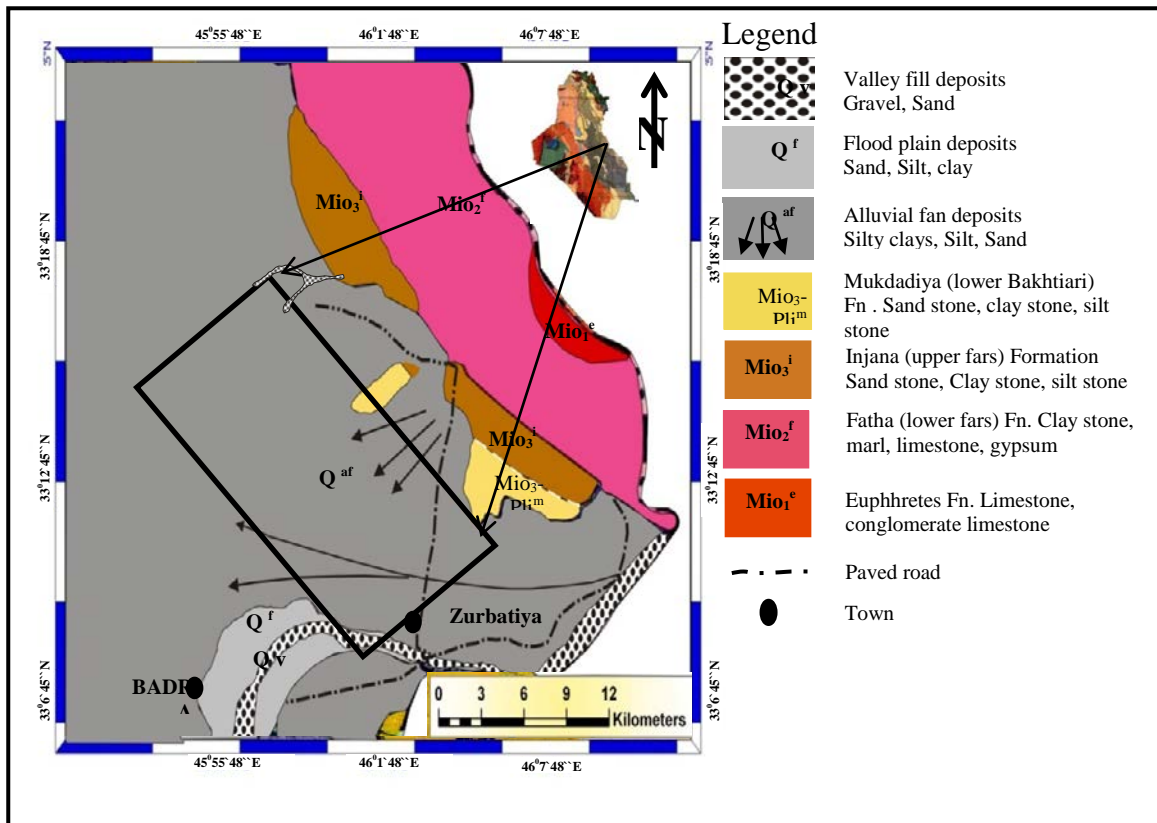


Figure 1- Geologic map of the study area [29].

Data acquisition

Eleven VES points distributed on two profiles were collected using Schlumberger array in the study area, figure 2-. The maximum current (AB) and potential (MN) electrodes spacing was (1400m) and (80m) respectively. The profile A-A' has (6) VES points with total length equal to (7.5km), while the total length of profile B-B' is (8.2km), and it has (5) VES points.

The 2D imaging survey was carried out using Wenner-Schlumberger array, because it is moderately sensitive to both horizontal (for low n-values) and vertical (for high n-values) geological structures. Also the median depth of investigation and horizontal coverage of this array are slightly better than the Wenner array [11].

Six (6) 2D stations were carried out in the study area as shown in figure 2-. The total length survey for each station was (1190m), 120 electrodes, and the electrode spacing was (10m), except for 2D station two (2DS2), which had a total length of (590m), 60 electrodes, and electrode spacing equal to (10m). The n-factor was setup as a maximum (6), because the larger n-factor and a-spacing give relatively deeper information of subsurface [12]. All VES points and 2D stations were applied on flat area in direction (NW-SE) parallel to the strike of layers using SYSCAL Pro+ resistivity meter.

Finally, it must be mentioned here that 2DS4 and 2DS6 are applied within profile A-A', where the 2DS4 is near well (BH2). 2DS3 and 2DS5 are applied within profile B-B' where 2DS3 is near (BH4). The 2DS1 and 2DS2 are conducted out of profiles near (BH5) and (BH6) respectively.

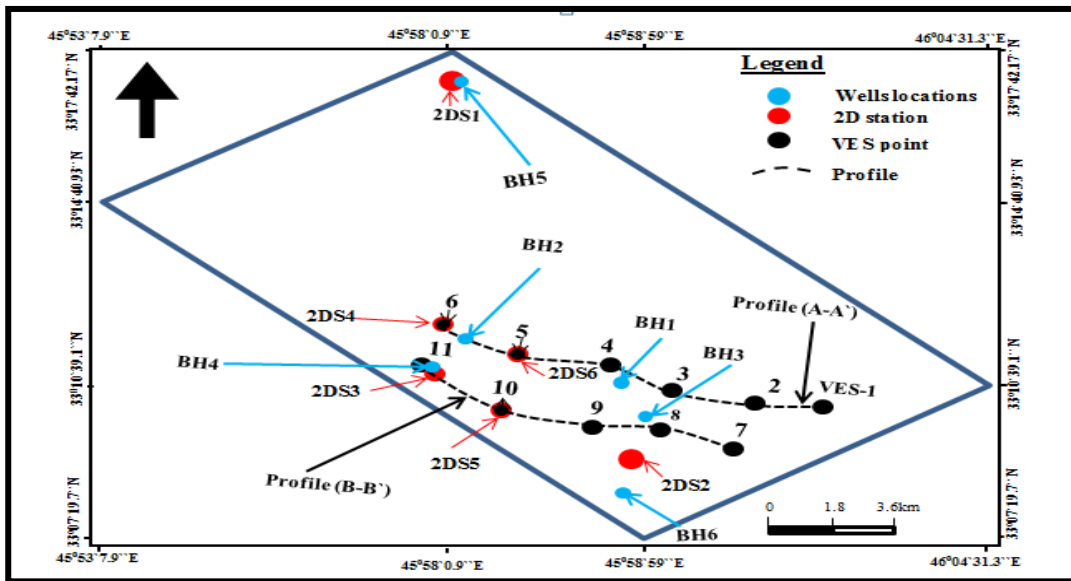


Figure 2- Location of 2D imaging stations and VES points

Results and discussion

a. Results and discussion of VES data

The VES points are plotted on a double-logarithm transparent graph sheet. The curves are interpreted manually using Ebert method [30, 31, 32], and also interpreted by using the inverse modeling method of IPI2Win software [33]. The results of inverse modeling are closest to manual interpretation. Therefore, the results of inverse modeling are used to construct two geoelectrical sections along profiles A-A` and B-B`, and then, with the help of the lithology of the wells, they are transformed to geological sections. They show the presence of six zones reflecting the presence of sand, gravel, silt, and clay layers of Quaternary deposits. The deposits indicate a decrease in their size in the middle of geological sections, as shown in the geological section of profile A-A`, and with depth. figure 3&4-, respectively.

The two geological sections show the presence of the Quaternary aquifer, which consists of sand (or gravel) and silt deposits with a resistivity range of (3-28Ωm). The decreasing resistivity values are related to the presence of salt groundwater and/or increasing clay content. The thickness of this aquifer increases toward SE and ranges between (30-200m). It occurs at a depth of (10-30). There is a sign of the geological section along profile B-B` indicating the presence of AL-Mukdadiya Formation. However, evidence of this, for example the presence of a deep well, is non-existent.

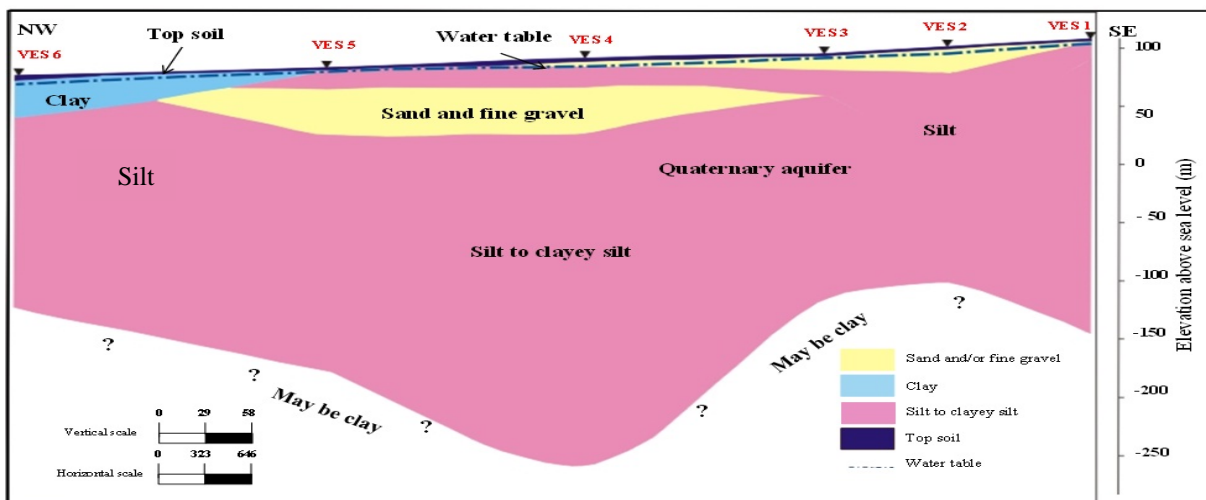


Figure 3- Shows the geological section along (A-A` profile).

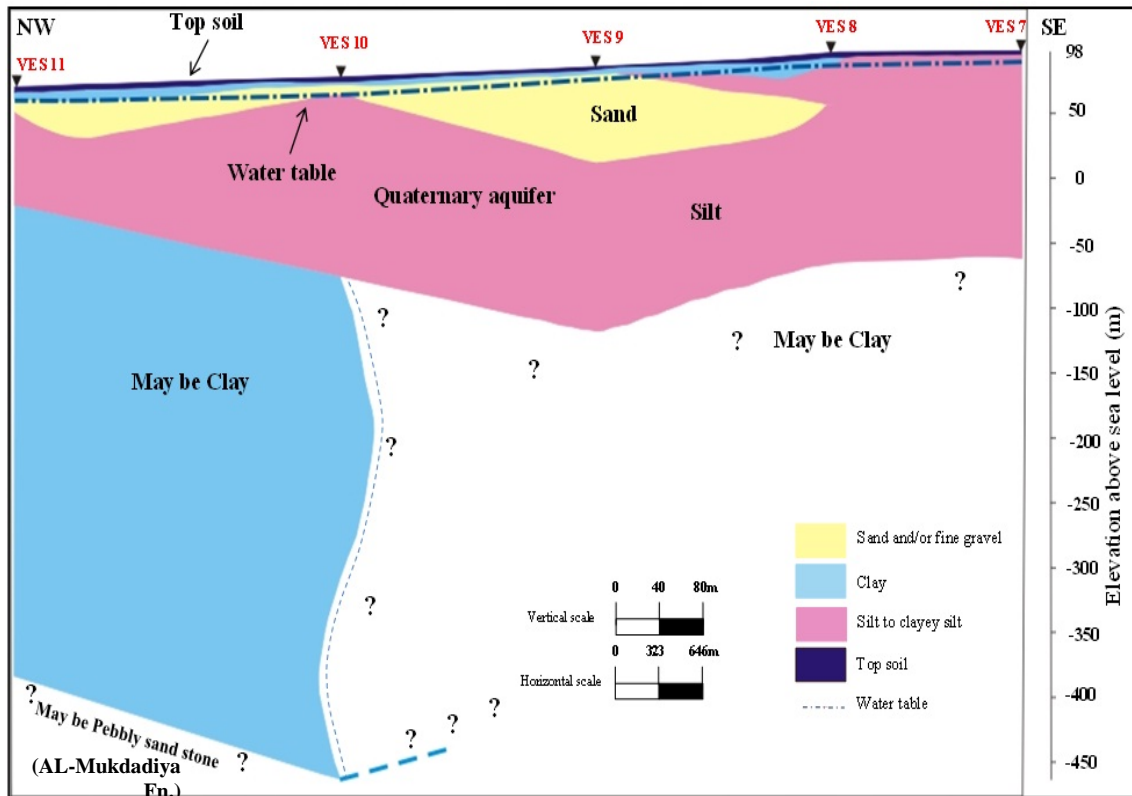


Figure 4- The geological section along (B-B') profile.

b. Results and discussion of 2D imaging data

The RES2DINV software [34] is used to interpret and create inverse models of measured data of the 2D stations. The results of interpretation are given in the following:

-The inverse model of 2DS1, figure 5- shows five major horizons reflecting five lithological layers as shown in BH5. However, this inverse model shows two aquifer types. The first is unconfined aquifer reflecting gravel, sand, silt, and clay of the Quaternary deposits and occurs at depth (10m). This aquifer has resistivity ranges between (1-55 Ωm) and thickness reaching (130m).

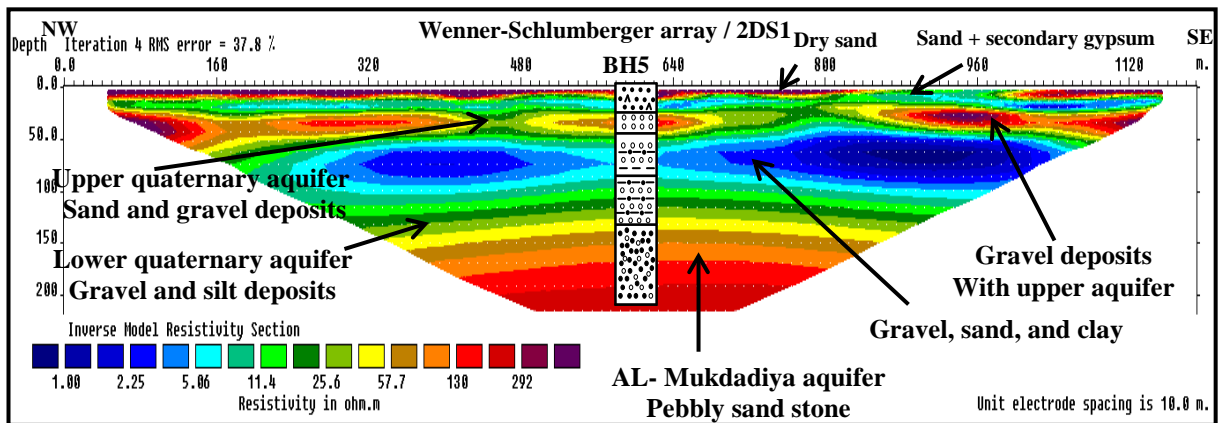


Figure 5- The inverse model of 2DS1.

The first aquifer can be separated into upper and lower Quaternary aquifers. The second aquifer is confined aquifer, which represents the pebbly sandstone of the AL-Mukdadiya Formation according to BH5. It has resistivity ranges between (57-292 Ωm). This aquifer occurs at a depth equal to (140m), while its thickness is more than (80m).

-The inverse model of 2DS2 shows the presence of five horizons. According to BH6, they are reflecting five lithological layers, figure 6-. The aquifer in this inverse model appears at depth between

(45-50m) and has a thickness between (35-55m). This aquifer reflects the presence of gravel layer of Quaternary deposits. Its resistivity values are ranging between (9.55-19.8 Ωm).

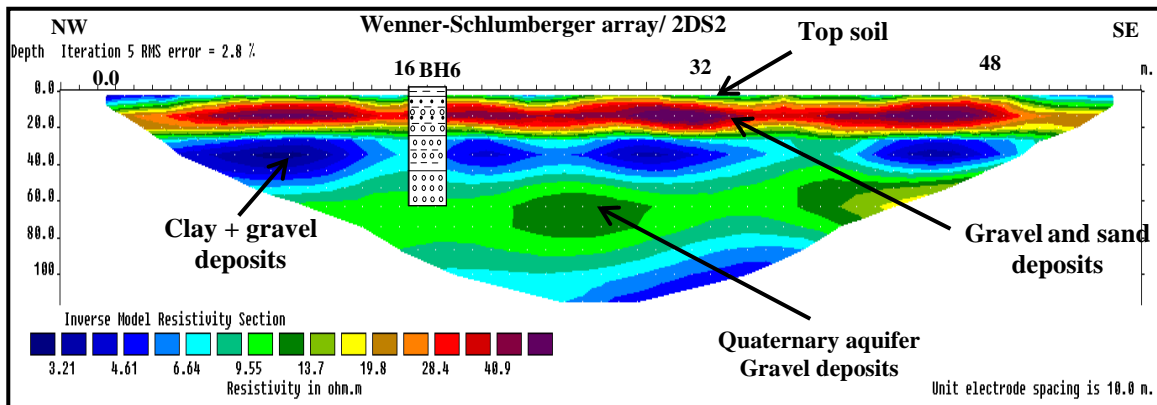


Figure 6- The inverse model of 2DS2.

- The inverse model of 2DS3 shows four horizons reflecting four lithological layers belonging to the Quaternary deposits, figure 7- according to BH4. The quaternary aquifer in this model is separated into upper and lower aquifers. The upper aquifer has resistivity ranging between (3Ωm) to more than (12 Ωm), and thicknesses between (60-100m). The lower aquifer occurs at a depth of about (190m) with unknown thickness. Its resistivity values range between (5Ωm) to more than (12Ωm). However, the lower aquifer dose not seen in the geological section along profile B-B` , figure 4-.

The interpretation of VES-11, which is located near electrode number (41) of 2DS3, indicates approximately coinciding with the resistivity values of 2D inverse model especially to depth of (90m). Beyond this depth, the VES-11 shows a very thick horizon with resistivity of (3.272 Ω.m) and thickness of (356.5), while the 2D inverse model shows a horizon with approximately the same resistivity, but with a thickness of (100m), which may reflect the presence of clay layer. This difference is accepted because, in 1D technique, the resistivity values of the horizons are calculated from an average of resistivity values. However, VES-11 may give a sign of the presence of AL-Mukdadiya deposits, which are not shown in 2DS3, because it has more depth investigation than that of the 2D technique.

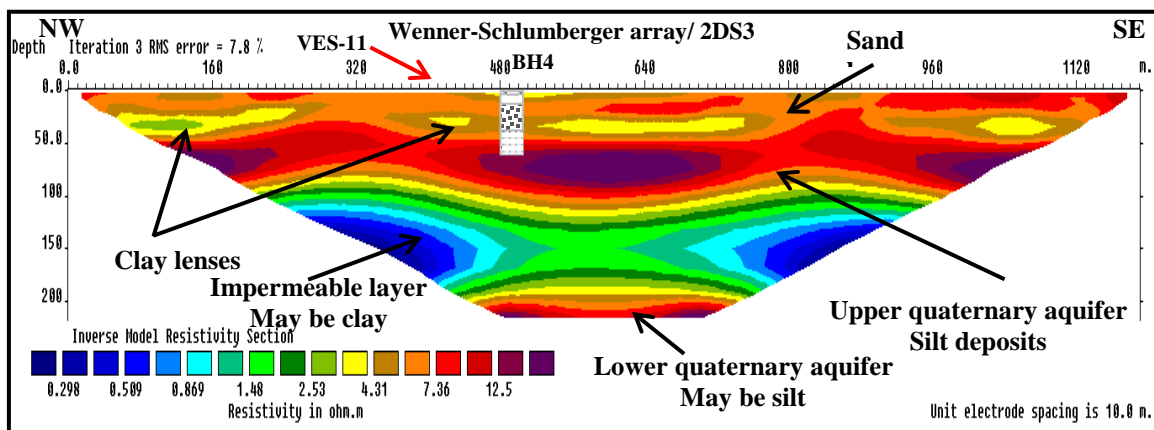


Figure 7- The inverse model of 2DS3.

- The inverse model of 2DS4 shows the presence four horizons, figure 8-. However, the third horizon represents silt deposits as shown in BH2, and it extends along the inverse model. The depth of this horizon reaches to (40), and its thickness ranges between (50m) to more than (180m). Its resistivity ranges between (6Ω.m) to more than (26Ω.m). This horizon is not shown in the geological section along profile (A-A`). This means that the 2D imaging technique is better than that of the 1D resistivity technique in delineating the aquifers and in determining the aquifers. This horizon can be considered as Quaternary aquifer. One note must be mentioned here, that the thickness of this aquifer increases

rapidly between electrodes number (55-61). as shown in the (2DS3), but the aquifer was separated into upper and lower Quaternary aquifer, figure 7-. In 2DS4 inverse model, the aquifer remains without separation, although its extent decreases by the fourth horizon intrusion. However, this is not evident in the inverse model of (2DS5) and (2DS6).

The interpretation of VES-6 indicates agreement with inverse model of (2DS4), although the first and second horizons of VES-6 do not appear in the model section. However, the VES-6 gives more depth of investigation (DOI) than that of the 2D imaging.

-The inverse model of 2DS5, figure 9- shows five horizons reflecting five lithological layers. The aquifer in this inverse model appears at depth (35-50m). It has variable thickness, which ranges between (50-90m), reflecting the presence of silt and/or sand layers belonging to the Quaternary deposits. Its resistivity ranges between (6Ωm) to more than (11Ωm).

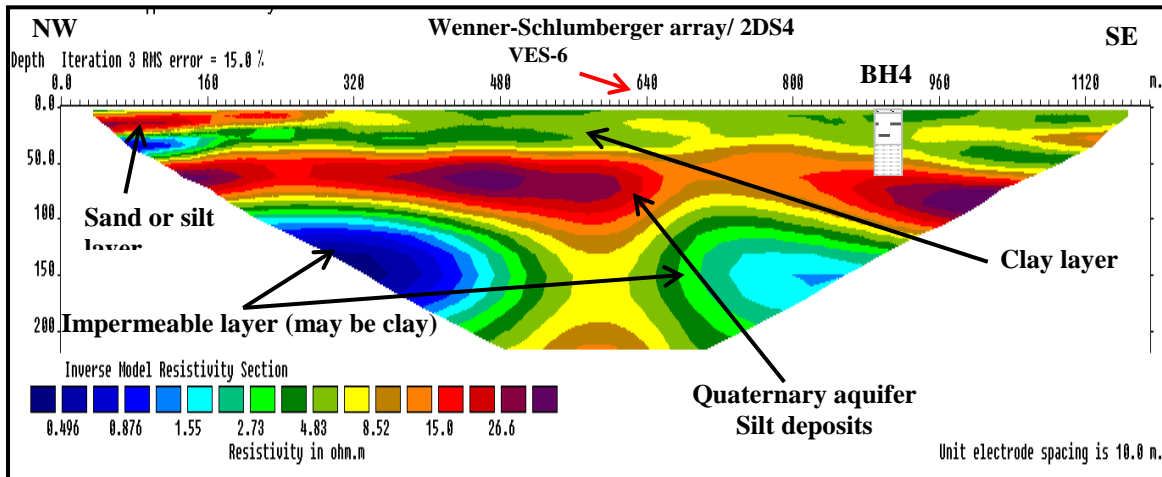


Figure 8- The inverse model of 2DS5.

The interpretation of VES-10, which occurs near electrode (64) of (2DS5), shows coincidence with the 2DS5 inverse model, figure 9-. However, the third horizon (clay lenses) in the inverse model does not appear in the interpretation of VES-10.

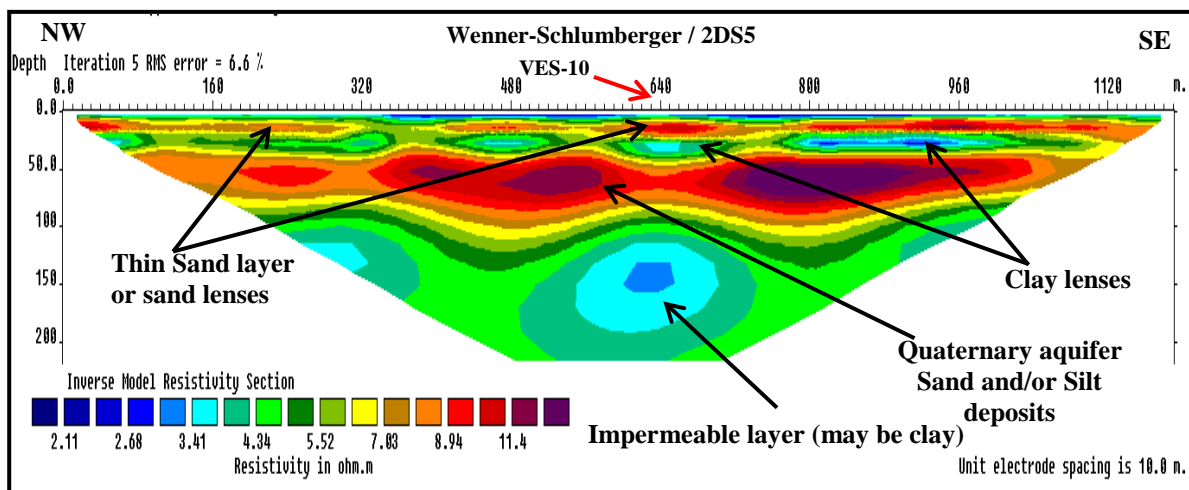


Figure 9- The inverse model of 2DS4.

This indicates that the 2D imaging technique is more accurate, and it is better at recognizing more layers or aquifers than that of the VES. It gives a more detailed picture of the subsurface than that of the VES resistivity technique.

- The inverse model of 2DS6 shows three major horizons, figure 10-. They reflect the presence of three major lithological layers belonging to the Quaternary deposits. The aquifer appears at a depth of

(40-65m), and its thickness ranges between (70-90m). This aquifer consists of silt and/or sand deposits. Its resistivity values are ranging between (7 Ω m) to more than (10 Ω m).

The interpretation of VES-5, which occurs near electrode number (64) of 2DS6, does not indicate accurate results. It shows thick horizon, about (200m) with resistivity equal to (7 Ω m), occurs at a depth of about (76m). While, the 2DS6 inverse model shows that there are two thick horizons. One occurs at a depth (50-65m) with thicknesses between (70-90m) and another with a thickness of more than (90m), and occurs at depth of about (140m). The cause of such a case in VES resistivity is the gradual decrease in resistivity with depth. However, in 2D imaging technique a huge amount of data is obtained, so it gives an accurate picture of subsurface and it is better in delineating the changes in resistivity with these layers.

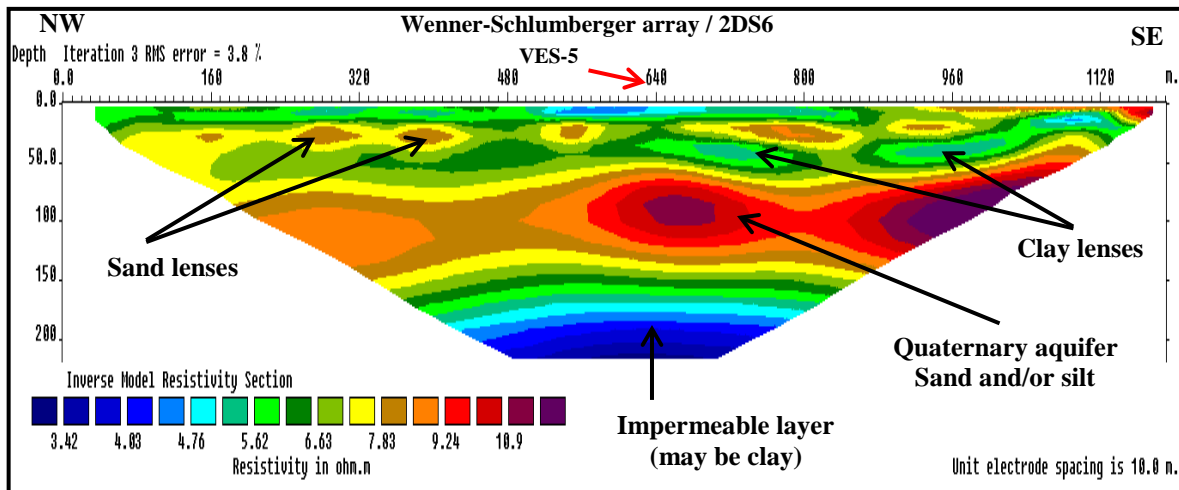


Figure 10- The inverse model of 2DS6.

Comparison between VES and 2D imaging techniques

1. The geological sections of VES technique succeeded in delineating the boundaries between layers. But, the invers models of 2D imaging technique are better in delineating the aquifers and in determining the vertical and horizontal changes in resistivity within layers and aquifers. Also, it succeeded in recognizing the upper and lower aquifers as shown in (2DS1), (2DS3), and (2DS4). Therefore, it is better at distinguishing more layers or aquifers than that of the VES.
2. The VES technique failed in detecting layers which have gradual decreases (or increases) in resistivity values or layers with small thicknesses. While, the 2D imaging technique succeeded in delineating these layers. This is shown in 2DS4, and 2DS3 in comparison with the geological section along profiles (A-A`), and (B-B`).
3. The VES survey gave a general view of the geological setting of subsurface horizons, while 2D imaging technique gave a detailed view of the subsurface geology. The 2D imaging required a huge amount of measurements, therefore it showed an accurate picture of lateral and vertical variation in lithology.
4. 1D resistivity technique indicated high DOI in comparison with 2D imaging technique. But, in 1D resistivity technique, this depth becomes uncontrolled, and it is difficult to determine whether the distance between electrodes is increasing, while in 2D imaging technique the DOI is controlled by huge data measurements.

Conclusion

The results of geological sections and invers models of 2D imaging stations showed the presence of two aquifers:

The first is the Quaternary aquifer, which appeared in all the geological sections and 2D imaging stations. This aquifer can be divided into upper and lower aquifers as shown in (2DS1), (2DS3), and (2DS4). In general, the thickness of this aquifer ranges between (30-200 m) which occurs at a depth of (10-30m), according to geological sections of VES survey, while it thickness varies between (35-180m) and occurs at a depth of (10-45m) according to invers models of 2D imaging survey.

The second is the AL-Mukdadiya aquifer, which appeared in 2DS1 only at a depth of (140m), and thickness exceeded (80m).

Acknowledgments

The authors would like to thank the general director of General Commission for Groundwater (Mr. Dhafir Abdullah) for providing requirements for achieving the field work, as well as offering all facilities to finish this work. Also, I would like to thanks (Dr. Ahmad Nadhum), the head of studies and investigation department, and (Mr. Dhia'a Basha) for their supporting.

My thanks to the geophysicists (Mr. Ahmed S. AL-Zubedi), (Dr. Firas H. AL-Menshed), and (Mr. Ahmed A. Al-Ibrahimi) for continues advices, and supporting in all work stages.

References

1. Kunetz, G., 1966. *Principle of direct current resistivity prospecting*. Borntrager, Berlin, pp: 103.
2. Koefoed, O., 1979. *Geosounding principles*, 1. Elsevier scientific publishing company. pp: 276.
3. Griffiths D.H. Barker R.D., 1993. Two-dimension resistivity imaging and modeling in area of complex geology, *Journal of Applied Geophysics* 29, pp: 211–226.
4. Loke, M.H. and Barker R.D., 1996a. Rapid least-squares inversion of apparent resistivity pseudo sections by a quasi-Newton method. *Geophysical Prospecting* 44, pp: 131–152.
5. Loke, M.H. and Barker, R.D., 1996b. Practical techniques for 3D resistivity surveys and data inversion. *Geophysical Prospecting* 44, pp 499-524.
6. Dahlin, T. and Bernstone, C., 1997. A roll-along technique for 3D resistivity data acquisition with multi-electrode array. *Proceedings of the Symposium on the Application of geophysics to Engineering and Environmental Problems*, Reno, Nevada, 2, pp: 927-935.
7. Dahlin, T., Bernstone, C., Loke, M.H., 2002. A 3-D resistivity investigation of a contaminated site at Lernacken, Sweden. *Geophysics* 67 (6), pp: 1692–1700.
8. Bentley, L.R., Gharibi, M., 2004. Two- and three-dimensional electrical resistivity imaging at a heterogeneous remediation site. *Geophysics* 69, pp: 674–680.
9. Dutta S, Krishnamurthy NS, Arora T, Rao VA, Ahmed S, Baltassat JM., 2006. Localization of water bearing fractured zones in a hardrock area using integrated geophysical techniques in Andhra Pradesh. *Hydrogeol J* 14, pp: 760–766.
10. Gunther, T., Rucker, C., Spitzer, K., 2006. Three-dimensional modeling and inversion of dc resistivity data incorporating topography-II. Inversion. *Geophysical Journal International* 166, pp: 506–517.
11. Loke, M. H., 2012. Tutorial: 2-D and 3D Electrical Imaging Surveys, pp.: 172, www.geotomosoft.com, www.geoelectrical.com.
12. Van Overmeeren R.A., 1989. Aquifer boundaries explored by geophysical measurements in the coastal plain of Yamen. A case of equivalence. *Geophysics* 54(1), pp: 38–48.
13. Medeiros W.E. Lima O.A.L., 1990. A Geoelectrical investigation for groundwater in crystalline terrains of central Bahia, Brazil. *Ground Water* 28(4), pp: 518–523.
14. Hago, H.A., 2000. Applied of electrical resistivity method in quantitative assessment of groundwater reserve of unconfined aquifer. M.Sc. Thesis, university of putra Malaysia. pp: 191.
15. Dahlin, T., and Zhou, B., 2004. Numerical comparison of 2D resistivity imaging with 10 electrode arrays. *Geophysical prospecting*, 52, pp: 379-398.
16. Amin, A. K., 2008. Aquifer delineation and evaluation of hydraulic parameters from surficial resistivity measurements in sharazoor basin- north east Iraq. PhD thesis, college of science, university of Baghdad, pp: 181.
17. Olugbenqa, A. F., 2009. Two dimensional shallow resistivity investigation of the groundwater potential at Nuhu Bamalli polytechnic, Zaria Main Campus using Electrical Imaging Technique. *The pacific Journal of science and technology*. 10 (1). pp: 602-613.
18. Kumar D., Rao V.A., Nagaiah E., Raju P.K., Mallesh D., Ahmeduddin M., Ahmed S. ,2010. Integrated geophysical study to decipher potential groundwater and zeolite-bearing zones in Deccan Traps. *Curr Sci* 98(6), pp: 803–814.
19. Nwankwo, L. I., 2011. 2D resistivity survey for groundwater exploration in hard rock terrain: A case study of Magdas observatory, Unilorin, Nigigeria, *Asian journal of earth science*, 4(1). pp:46-53.

20. AL-Shemmari, A. N. H., **2012**. Establishing relations between hydraulic parameters and geoelectrical properties for fractured rock aquifer in Dammam formation at Bahr-AL-Najaf Basin. PhD thesis, College of science, University of Baghdad, pp: 160.
21. Ratnakumari Y., Rai S.N., Thiagarajan S., Kumar D., **2012**. 2Electrical resistivity imaging for delineation of deeper aquifers in a part of the Chandrabhaga river basin, Nagpur District, Maharashtra, India. *Curr Sci* 102(1), pp:61–69.
22. Ayolabi, E. A., Folorunso, A. F., Eleyinimi, A. F., **2009**. Applications of 1D and 2D Electrical Resistivity Methods to Map Aquifers in a Complex Geologic Terrain of Foursquare Camp, Ajebo, Southwestern Nigeria. *The pacific journal of science, and technology*, 10| (2), pp:657-666.
23. AL-Zubedi, A. S., and Thabit, J. M., **2012**. Comparison between 2D imaging and vertical electrical sounding in aquifer delineation: a case study of south and south west of Samawa City (IRAQ). *Arabian Journal of Geosciences*. DOI. 10. pp: 8.
24. AL-Jiburi. H. K. S., **2006**. *Hydrogeological and hydrochemical study of Mandali quadrangle*. State company of geological survey and mining. 56p.
25. Jassim. S. Z., Goof. J. C., **2006**. *Geology of Iraq*. Dolin, Prague and Moravian Museum, Brno, Czech Republic. pp: 337.
26. Jassim. H. K., **2009**. Petrography and sedimentology of AL-Mukdadiya Formation in Badra area eastern-Iraq. M.Sc. Thesis, College of science, University of Baghdad, pp: 142.
27. AL-Azawi. B. M. A., **2002**. Hydrogeological properties of ground water system in Badra-Jassan Basin. M.Sc. Thesis, College of science. University of Baghdad, pp: 97.
28. AL-Shammary. S.H.E., **2008**. Hydrogeology of Galal Basin-wasit-east Iraq. PhD thesis, College of science. University of Baghdad, pp: 145.
29. State Company of geological survey and mining, **1996**. geological map of Iraq, Baghdad, Iraq.
30. Keller, G.V., and Frischknecht, F.C., **1966**. *Electrical methods in geophysical prospecting*. Pergamon press, New York. pp: 319.
31. Orellana, E., and Mooney, H. M., **1966**. *Master tables and curves for vertical electrical sounding over layered structures*. Interciencia Madrid.
32. Battacharya, P.K., and Petra, H.P., **1968**. *Direct current geoelectrical sounding*. Elsevier publishing Co. Amsterdam. pp: 131.
33. Moscow, 2001. *IPI2win V. 2. 1, IPI_Res2, IPI_Res3, user's guide*. Geological Faculty, Dept. of Geophysics, Moscow state university, pp: 25.
34. Geotomo software, **2008**. *RES2DINV version 3.57, Rapid 2D resistivity and IP inversion using the least squares method*, Penang, Malaysia, pp: 148.